Estimation of Movement Speed in Monitoring Systems based on Sensors of Multiple Types

Jakub Wagner[a] and Paweł Mazurek[b]
Institute of Radioelectronics and Multimedia Technology, Warsaw University of Technology, Warsaw, Poland

Keywords: Healthcare, Monitoring, Data Fusion, Numerical Differentiation, Regularisation, Total Variation.

Abstract: The research reported in this paper is related to the differentiation and fusion of measurement data in systems for healthcare-oriented unobtrusive monitoring of elderly persons. Two methods for regularised numerical differentiation – suitable for different shapes of trajectories of the monitored person's movement – are considered. A technique for the fusion of data from sensors of different types – which involves weighting those data according to the available *a priori* information about the variances of errors corrupting those data – is presented. Guidelines on the usage and optimisation of that technique are provided according to the results of numerical experimentation based on synthetic data.

1 INTRODUCTION

1.1 Motivation for Monitoring

The life expectancy at birth, estimated for the global population in 2019, is *ca.* 73 years; it has been rising during the last decades and is predicted to reach 77 years by the half of the twenty-first century, while the global fertility rate – *i.e.* the number of live births per woman over a lifetime – is decreasing (United Nations, 2019). For these reasons, the global population is ageing, *i.e.* the share of people aged at least 65 years is growing. Taking into account these predictions, several global institutions involved in the protection and management of public health have pointed out the necessity to take actions aimed at improving the quality of life of elderly people and at ensuring that the public expenditures, related to the healthcare services addressed to those people, remain affordable (see, for example, WHO, 2017). That necessity has inspired the development of diverse technological means, designed to facilitate the accomplishment of various healthcare-related objectives such as the reduction of the number of admissions to nursing homes, the optimisation of the processes of treatment or rehabilitation, or the social integration of elderly people. For instance:

- Alerting devices – such as those worn on the body or clothes, which send out an emergency signal when a button is pressed – reduce the delay of intervention after dangerous events such as falls, and enhance the sense of safety of elderly people who live independently in their households, thus encouraging them to stay active (Fleming and Brayne, 2008).
- Robots support elderly people in tasks which they are unable to complete without aid, and may relieve them from the sense of loneliness (Wada et al., 2004, Sharkey and Sharkey, 2012).
- Sensors and actuators ensuring the safe functioning of household appliances protect elderly people from dangerous accidents (Al-Shaqi et al., 2016).
- Video games which involve players in physical activity may be used to promote such activity among elderly people and gather information about their health status (Garcia Marin, 2015).
- Social-networking websites and systems based on ambient-display screens – designed to help elderly people maintain contact with their relatives and friends – help prevent their social isolation (Campos et al., 2016).
- Monitoring systems provide data representative of the behaviour and physiological parameters of independently-living elderly people, help in identifying progressive changes in those people's health

[a] https://orcid.org/0000-0002-2739-4578
[b] https://orcid.org/0000-0002-8239-4589

Wagner, J. and Mazurek, P.
Estimation of Movement Speed in Monitoring Systems based on Sensors of Multiple Types.
DOI: 10.5220/0010249300690079
In *Proceedings of the 14th International Joint Conference on Biomedical Engineering Systems and Technologies (BIOSTEC 2021) - Volume 4: BIOSIGNALS*, pages 69-79
ISBN: 978-989-758-490-9

status and enable quick reactions to dangerous accidents (Peetoom et al., 2015).

This study is focused on technological solutions belonging to the last category, *viz.* on monitoring systems which enable the acquisition of data representative of the monitored person's movement trajectory. Such data can be used to obtain information useful for the healthcare practitioners, in particular – to estimate the monitored person's walking speed. Walking is a complex task which requires the interaction of several organs and the proper functioning of multiple parts of the brain (Kikkert et al., 2016). The analysis of gait can provide information about the so-called *functional mobility*, *i.e.* a set of abilities related to balance and gait manoeuvres used in everyday life – abilities which partially reflect the overall health status (Shumway-Cook et al., 2000). Some quantities characterising the gait – such as the stride length, the stride frequency, or the variability of the stride time – are correlated with the risk of falling and are useful as indicators of conditions such as Parkinson's disease, osteoarthritis or diabetes (Hodgins, 2008). On the other hand, the speed with which a person walks comfortably during every-day activities – the so-called *self-selected walking speed* – has been recently recognised as a versatile, informative and easily measurable indicator of functional mobility and general health status (Lusardi, 2012):

- its values smaller than 0.6 m/s indicate a high risk of fall and hospitalisation;
- its increase of at least 0.1 m/s is a useful predictor of well-being;
- its similar decrease is correlated with the deterioration of the health status or the decline in overall functioning.

In clinical settings, self-selected walking speed can be estimated by using a stopwatch to measure the time which the examined person needs to walk along a path of a predefined length; however, the in-home use of monitoring systems may prove to be more reliable, convenient and affordable than clinical assessment sessions (Hagler et al., 2010).

Apart from the estimation of the self-selected walking speed, the data representative of the monitored person's two- or three-dimensional movement trajectory – together with the estimates of velocity and acceleration, obtained on the basis of those data – can be used in other healthcare-oriented applications, such as the detection of falls (Khan and Hoey, 2017) or the analysis of that person's behavioural patterns (Baldewijns et al., 2016), which may enable the early detection of the onset of dementia.

1.2 Techniques for Monitoring

In the practice of healthcare-oriented monitoring, the solutions based on wearable sensors – *i.e.* sensors attached to the body or clothes of the monitored person, including accelerometers, gyroscopes and sensors of physiological parameters – are the most widespread ones (Majumder et al., 2017). The most important drawback of such techniques is the fact that the need to wear devices may be considered inconvenient by the people subject to monitoring; furthermore, a system based on wearable devices becomes useless if the monitored person forgets to wear the device or decides not to do it. For these reasons, it seems desirable to develop monitoring systems which do not require any action from the monitored persons.

Other monitoring techniques, already applied in healthcare practice, include those based on video cameras, passive-infrared detectors of motion and pressure sensors. There are also two emerging categories of monitoring techniques which attract growing attention of researchers, *viz.* techniques based on depth sensors and impulse-radar sensors. The recent attempts to apply them for monitoring of elderly persons are mainly motivated by the conviction that they may be less intrusive, invasive and cumbersome than the above-mentioned, better explored techniques.

This study is devoted to the monitoring techniques which – like those based on depth sensors and impulse-radar sensors – involve the estimation of the position of the monitored person's centre of mass with high temporal resolution (*i.e.* several to several dozen estimates per second), followed by the analysis of the sequences of those estimates. Such techniques require numerical differentiation in order to estimate the monitored person's movement speed. The position estimates are corrupted with measurement errors, so their numerical differentiation is an ill-posed problem, *i.e.* if no remedies are applied, small errors corrupting the data may cause large errors in the speed estimates. Therefore, the problem of numerical differentiation needs to be regularised, *i.e.* redefined in such a way as to ensure a kind of "regularity" of the speed estimates, at the cost of limiting their attainable fidelity to the measurement data, in order to reduce their sensitivity to the measurement errors.

Sensors which operate according to different physical principles tend to have specific complementary advantages and disadvantages; for example, impulse-radar sensors offer a broad field of view and the capacity of through-the-wall monitoring, but provide estimates of the monitored person's position corrupted with larger errors than depth sensors, which – on the other hand – cannot detect occluded persons and whose field of view is limited. This study is devoted to monitoring systems which employ sensors of multiple types and thus require the application of an adequate method for the fusion of data acquired by means of those sensors.

Despite the generally recognised need for developing technological solutions aimed at improving the quality of life of elderly people and contributing to the efficiency of public health management, healthcare-oriented monitoring systems are still not being commonly used in healthcare facilities and households. This may be explained by the difficulties related to the development of technological solutions which can be both widely accepted among elderly people and – at the same time – capable of providing healthcare practitioners with useful information (Debes et al., 2016). Solutions aimed at combining the complementary advantages of several types of sensors seem to have a promising potential for achieving a satisfactory compromise between the two above-mentioned qualitites.

1.3 Scope of Study

Two methods of numerical differentiation have been considered in this study (*cf.* Subsection 2.2):

- a method based on Tikhonov regularisation, suitable for the analysis of smooth movement trajectories;
- a method based on total-variation regularisation, suitable for the analysis of piecewise-linear movement trajectories.

In both cases, the fusion of data from different sensors has been performed by adopting an adequate indicator of the fidelity of the speed estimates to the measurement data (*cf.* Subsection 2.3). The aim of this study is the analysis of the properties and applicability of that indicator – the analysis based on the results of experiments performed using synthetic data.

2 ESTIMATION OF MOVEMENT SPEED

2.1 Mathematical Formulation of Research Problem

Let's assume that the time-dependence of the monitored person's position in a given direction can be modelled using a scalar, real-valued function $f:\mathbb{R}\to\mathbb{R}$ of a scalar variable t modelling time, differentiable on the interval $[0,T]$. The analytic form of f is unknown. The available data $\tilde{x}_1,\ldots,\tilde{x}_N$ are its error-corrupted values, resulting from measurements performed at time instants $t_1,\ldots,t_N$ such that $0=t_1<\cdots<t_N=T$. Those data are modelled as follows:

$$\tilde{x}_n = f(t_n)+\eta_n \quad \text{for} \quad n=1,\ldots,N \tag{1}$$

where $\eta_1,\ldots,\eta_N$ are realisations of independent random variables $\underline{\eta}_1,\ldots,\underline{\eta}_N$ modelling measurement errors. Since it is assumed that those data may have been acquired by means of different types of sensors, the distributions of the variables $\underline{\eta}_1,\ldots,\underline{\eta}_N$ may differ; in this study, it is assumed that those variables are zero-mean, normally distributed and that their variances are $\sigma_1^2,\ldots,\sigma_N^2$. Those variances are unknown, but their estimates $\hat{\sigma}_1^2,\ldots,\hat{\sigma}_N^2$ are available; in practice, these estimates may be obtained as a result of prior calibration experiments.

The time-dependence of the monitored person's speed in the given direction is modelled with $f^{(1)}$, *i.e.* the first derivative of f. Speed estimates $\hat{x}_1^{(1)},\ldots,$ $\hat{x}_N^{(1)}$ are sought such that:

$$\hat{x}_n^{(1)} \cong f^{(1)}(t_n) \quad \text{for} \quad n=1,\ldots,N \tag{2}$$

2.2 Numerical Differentiation

The procedure for numerical differentiation, *i.e.* determination of the sequence $\hat{x}_1^{(1)},\ldots,\hat{x}_N^{(1)}$ on the basis of the sequence $\tilde{x}_1,\ldots,\tilde{x}_N$, involves the following operations:

- approximation of the function f,
- computation of the first derivative $\hat{f}^{(1)}$ of the result of approximation $\hat{f}$,
- evaluation of $\hat{f}^{(1)}$ at the time instants $t_1,\ldots,t_N$.

The approximation of f requires the determination of a set of admissible approximating functions and the selection of one of them on the basis of the data $\tilde{x}_n$. In this study, it is assumed that the admissible approximating functions are polynomial splines of degree 2. Such functions are defined as quadratic polynomials in each subinterval $[t_n,t_{n+1}]$, $n=1,\ldots,N-1$; hence, it can be easily checked that the following equality is satisfied for each such function $\hat{f}$:

$$\hat{f}(t_n) - \hat{f}(t_{n-1}) = \left[\hat{f}^{(1)}(t_n) + \hat{f}^{(1)}(t_{n-1})\right]\frac{t_n - t_{n-1}}{2} \quad \text{for} \quad n = 2, \ldots, N \tag{3}$$

Thus:

$$\hat{f}(t_n) - \hat{f}(t_1) = \hat{f}^{(1)}(t_n)\tfrac{t_n - t_{n-1}}{2} + \sum_{\nu=2}^{n-1}\hat{f}^{(1)}(t_\nu)\tfrac{t_{\nu+1} - t_{\nu-1}}{2} + \hat{f}^{(1)}(t_1)\tfrac{t_2 - t_1}{2} \quad \text{for} \quad n = 2, \ldots, N \tag{4}$$

The $N-1$ equations obtained by evaluating Eq. (4) for $n = 2, \ldots, N$ – the equations specifying the linear relation between the values of the approximating function and the values of its first derivative – may be supplemented by adopting an additional assumption regarding the movement of the monitoring person; here, it has been assumed that the speed of the monitored person is constant at the beginning of the time interval under analysis, *i.e.*:

$$\hat{f}^{(1)}(t_1) - \hat{f}^{(1)}(t_2) = 0 \tag{5}$$

Eq. (4) and Eq. (5) may be collected in the following way:

$$\mathbf{Q}\hat{\mathbf{x}}^{(1)} = \hat{\mathbf{x}}' \tag{6}$$

where $\hat{\mathbf{x}}'$ is the vector of values of the approximating function, shifted by $-\hat{f}(t_1)$:

$$\hat{\mathbf{x}}' \equiv \left[\hat{f}(t_1) - \hat{f}(t_1) \;\; \hat{f}(t_2) - \hat{f}(t_1) \cdots \hat{f}(t_N) - \hat{f}(t_1)\right]^{\mathrm{T}}$$

$\hat{\mathbf{x}}^{(1)}$ is the vector of estimates of the first derivative:

$$\hat{\mathbf{x}}^{(1)} \equiv \left[\hat{x}_1^{(1)} \cdots \hat{x}_N^{(1)}\right]^{\mathrm{T}} \equiv \left[\hat{f}^{(1)}(t_1) \;\cdots\; \hat{f}^{(1)}(t_N)\right]^{\mathrm{T}}$$

and the matrix $\mathbf{Q}$ is defined as follows:

$$\mathbf{Q} \equiv \begin{bmatrix} 1 & -1 & 0 & \cdots & \\ \frac{t_2 - t_1}{2} & \frac{t_2 - t_1}{2} & 0 & \cdots & \\ \frac{t_2 - t_1}{2} & \frac{t_3 - t_1}{2} & \frac{t_3 - t_2}{2} & 0 & \cdots \\ \vdots & & & \ddots & \\ \frac{t_2 - t_1}{2} & \frac{t_3 - t_1}{2} & \frac{t_4 - t_2}{2} & \cdots & \frac{t_N - t_{N-1}}{2} \end{bmatrix} \in \mathrm{R}^{N \times N}$$

If the measurement errors are negligible and – consequently – one may assume that the best approximating function is the one which interpolates the measurement data, *i.e.* $\hat{f}(t_n) = \tilde{x}_n$ for $n = 1, \ldots, N$, then Eq. (6) can be used directly to obtain the vector $\hat{\mathbf{x}}^{(1)}$ of speed estimates, *viz.*:

$$\hat{\mathbf{x}}^{(1)} = \mathbf{Q}^{-1}\tilde{\mathbf{x}}' \tag{7}$$

where $\tilde{\mathbf{x}}'$ is the vector of measurement data shifted by $-\tilde{x}_1$:

$$\tilde{\mathbf{x}}' \equiv \left[\tilde{x}_1 - \tilde{x}_1 \quad \tilde{x}_2 - \tilde{x}_1 \;\cdots\; \tilde{x}_N - \tilde{x}_1\right]^{\mathrm{T}}$$

However, the condition number of $\mathbf{Q}$ tends to be very large even for relatively small *N*, and thus the speed estimates obtained this way are unacceptably inaccurate even when the errors corrupting the data are small. The remedy for this is regularisation, which consists in imposing an additional constraint on the set of admissible approximating functions. Such a constraint should be based on a realistic *a priori* assumption regarding the movement of the monitored person, in particular – an assumption about the shape of the function f modelling the trajectory of that movement. In this study, constraints on the following two quantities are considered:

- the squared 2-norm of the vector of values of the second derivative of the approximating function, denoted with ρ hereinafter:

$$\rho \equiv \left\|\hat{\mathbf{x}}^{(2)}\right\|_2^2 \equiv \sum_{n=1}^{N}\left(\hat{f}^{(2)}(t_n)\right)^2 = \left\|\mathbf{D}\hat{\mathbf{x}}^{(1)}\right\|_2^2 \tag{8}$$

where $\hat{\mathbf{x}}^{(2)} \equiv \left[\hat{f}^{(2)}(t_1) \cdots \hat{f}^{(2)}(t_N)\right]^{\mathrm{T}}$ and:

$$\mathbf{D} \equiv \begin{bmatrix} \frac{-1}{t_2 - t_1} & \frac{1}{t_2 - t_1} & 0 & \cdots & \\ 0 & \frac{-1}{t_3 - t_2} & \frac{1}{t_3 - t_2} & 0 & \cdots \\ & \ddots & \ddots & & \\ & \cdots & 0 & \frac{-1}{t_N - t_{N-1}} & \frac{1}{t_N - t_{N-1}} \end{bmatrix} \in \mathrm{R}^{(N-1) \times N}$$

- the squared 1-norm of the vector of values of the second derivative of the approximating function, denoted with θ hereinafter:

$$\theta \equiv \left\|\hat{\mathbf{x}}^{(2)}\right\|_1^2 \equiv \left(\sum_{n=1}^{N}\left|\hat{f}^{(2)}(t_n)\right|\right)^2 = \left\|\mathbf{D}\hat{\mathbf{x}}^{(1)}\right\|_1^2 \tag{9}$$

The imposition of a constraint on ρ – being a variant of the regularisation technique commonly referred to as *Tikhonov regularisation* (Stickel, 2010) – is suitable when the monitored person's movement trajectory is adequately modelled with a smooth function, *i.e.* a function whose several derivatives are continuous. Such an assumption about the shape of the modelling function seems reasonable when human movement is analysed in a relatively short time interval; for example, during gait, the position of the monitored person's centre of mass along the direction orthogonal to the walking direction fluctuates smoothly with a period corresponding to the stride duration.

On the other hand, the imposition of a constraint on θ – being a variant of the regularisation technique commonly referred to as *total-variation* (TV) *regularisation* (Rudin et al., 1992) – is suitable when the movement trajectory is adequately modelled with a piecewise-linear function. Such an assumption seems reasonable when the walking trajectory is modelled in a time interval of several seconds or minutes, since people tend to walk with approximately piecewise-constant speed.

The effects of both considered regularisation techniques are illustrated in Figure 1, which presents the shapes of some arbitrarily selected, exemplary functions, characterised by different values of ρ and θ.

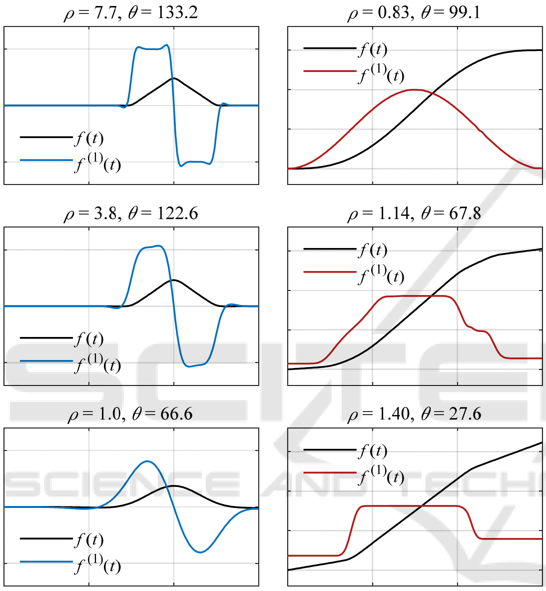

Figure 1: Exemplary functions, characterised by different values of ρ and θ, together with their first derivatives; the functions presented in the left column have been obtained by imposing decreasing constraints on ρ (note that θ also decreases); the functions presented in the right column have been obtained by imposing decreasing constraints on θ (note that in this case ρ increases).

For practical choices of the constraints ρ_{max} and θ_{max}, it is unlikely that there exists an admissible approximating function which satisfies such a constraint and – at the same time – interpolates the measurement data. Therefore, the vector of speed estimates needs to be determined by minimising an indicator of the fidelity of the results to the measurement data, denoted hereinafter with J; in the case of Tikhonov regularisation, this minimisation problem can be formulated in the following way:

$$\hat{\mathbf{x}}^{(1)} \equiv \arg_{\xi} \inf\left\{J(\xi) \mid \xi \in \mathrm{R}^N, \|\mathbf{D}\xi\|_2^2 \le \rho_{max}\right\} \quad (10)$$

and, analogously, in the case of TV regularisation:

$$\hat{\mathbf{x}}^{(1)} \equiv \arg_{\xi} \inf\left\{J(\xi) \mid \xi \in \mathrm{R}^N, \|\mathbf{D}\xi\|_1^2 \le \theta_{max}\right\} \quad (11)$$

Various choices for the indicator J are viable; the one studied here is described in the next subsection.

2.3 Fusion of Data from Different Sensors

In order to quantify the discrepancy between the results of estimation and the measurement data, one may evaluate the vector of approximation residuals, computed in the following way:

$$\hat{\mathbf{x}} - \tilde{\mathbf{x}} = \mathbf{Q}\hat{\mathbf{x}}^{(1)} - \tilde{\mathbf{x}}' \quad (12)$$

The *a priori* information about the accuracy of the employed sensors – the information contained in the estimates $\hat{\sigma}_1^2, \ldots, \hat{\sigma}_N^2$ – can be incorporated in the procedure for estimation of movement speed by allowing for larger approximation residuals at the time instants which correspond to the data acquired using sensors with lower accuracy. This can be done by defining the indicator J in Eq. (10) and Eq. (11) as a weighted norm of the vector $\hat{\mathbf{x}} - \tilde{\mathbf{x}}$, with weights selected on the basis of the estimates $\hat{\sigma}_1^2, \ldots, \hat{\sigma}_N^2$:

$$J \equiv \|\hat{\mathbf{x}} - \tilde{\mathbf{x}}\|_{\mathbf{W}}^2 \equiv \left\|\mathbf{Q}\hat{\mathbf{x}}^{(1)} - \tilde{\mathbf{x}}'\right\|_{\mathbf{W}}^2 = \\ = \left(\mathbf{Q}\hat{\mathbf{x}}^{(1)} - \tilde{\mathbf{x}}'\right)^{\mathrm{T}} \mathbf{W} \left(\mathbf{Q}\hat{\mathbf{x}}^{(1)} - \tilde{\mathbf{x}}'\right) \quad (13)$$

where $\mathbf{W} \in \mathrm{R}^{N \times N}$ is a diagonal weighting matrix whose *n*th element is defined as follows:

$$w_n = \hat{\sigma}_n^{-\beta} \Big/ \max\left\{\hat{\sigma}_\nu^{-\beta} \,\Big|\, \nu = 1, \ldots, N\right\} \quad (14)$$

with $0 \le \beta \in \mathrm{R}$ being a parameter controlling the amount of weighting. For $\beta = 0$, all the data are taken into account with equal weights; for larger β, the data corresponding to smaller $\hat{\sigma}_n^2$ (*i.e.* the data acquired using more accurate sensors) have more influence on the estimates of speed. The division by the maximum element in Eq. (14) ensures that $\|\mathbf{W}\|_2 = 1$, so that the values of J are in approximately the same range regardless of the value of β.

The experiments described in Section 3 are aimed at assessing the influence of the value of β and of the accuracy of the estimates $\hat{\sigma}_n^2$ on the quality of the estimates of speed.

2.4 Computational Formulae

Equation (10), defining the vector of speed estimates obtained using Tikhonov regularisation, can be reformulated using the Lagrange multiplier technique in the following way:

$$\hat{\mathbf{x}}^{(1)} = \arg_{\xi}\inf\left\{\left\|\mathbf{Q}\xi - \tilde{\mathbf{x}}'\right\|_{\mathbf{W}}^2 + \alpha\left\|\mathbf{D}\xi\right\|_2^2 \,\middle|\, \xi \in \mathrm{R}^N\right\} \tag{15}$$

where α is a regularisation parameter (related to the constraint $\rho_{\max}$) whose value may be selected empirically. The analytic solution of Eq. (15) yields:

$$\hat{\mathbf{x}}^{(1)} = \left(\mathbf{Q}^{\mathrm{T}}\mathbf{W}\mathbf{Q} + \alpha\mathbf{D}^{\mathrm{T}}\mathbf{D}\right)^{-1}\mathbf{Q}^{\mathrm{T}}\mathbf{W}\tilde{\mathbf{x}}' \tag{16}$$

In the case of TV regularisation, the corresponding minimisation problem – defined by Eq. (11) – can be reformulated in an analogous way, *viz.*:

$$\hat{\mathbf{x}}^{(1)} = \arg_{\xi}\inf\left\{\left\|\mathbf{Q}\xi - \tilde{\mathbf{x}}'\right\|_{\mathbf{W}}^2 + \alpha\left\|\mathbf{D}\xi\right\|_1^2 \,\middle|\, \xi \in \mathrm{R}^N\right\} \tag{17}$$

but the dependence of $\hat{\mathbf{x}}^{(1)}$ on $\tilde{\mathbf{x}}'$ cannot be expressed in closed form, because the term $\left\|\mathbf{D}\xi\right\|_1^2$ is not differentiable. However, $\hat{\mathbf{x}}^{(1)}$ can be determined using the following iterative algorithm, being a generalised version of the algorithm described in (Chartrand, 2011) (which corresponds to $\mathbf{W}$ being the identity matrix):

$$\hat{\mathbf{x}}_0^{(1)} \equiv \left[0 \cdots 0\right]^{\mathrm{T}} \tag{18}$$

$$\hat{\mathbf{x}}_{i+1}^{(1)} = \hat{\mathbf{x}}_i^{(1)} + \Delta\hat{\mathbf{x}}_i^{(1)} \quad \text{for} \quad i = 0, 1, 2, \ldots \tag{19}$$

where $\Delta\hat{\mathbf{x}}_i^{(1)}$ is the solution of the following set of linear algebraic equations:

$$\mathbf{H}\Delta\hat{\mathbf{x}}_i^{(1)} = -\mathbf{g}_i \tag{20}$$

$$\mathbf{H}_i \equiv \mathbf{Q}^{\mathrm{T}}\mathbf{W}\mathbf{Q} + \alpha\mathbf{D}^{\mathrm{T}}\mathbf{E}_i\mathbf{D} \tag{21}$$

$$\mathbf{g}_i \equiv \mathbf{Q}^{\mathrm{T}}\mathbf{W}\left(\mathbf{Q}\hat{\mathbf{x}}_i^{(1)} - \tilde{\mathbf{x}}'\right) + \alpha\mathbf{D}^{\mathrm{T}}\mathbf{E}_i\mathbf{D}\hat{\mathbf{x}}_i^{(1)} \tag{22}$$

with $\mathbf{E}_i \in \mathrm{R}^{(N-1)\times(N-1)}$ being a diagonal matrix whose nth element is defined as follows:

$$e_{i,n} \equiv \frac{1}{\sqrt{\left(\hat{x}_{i,n+1}^{(1)} - \hat{x}_{i,n}^{(1)}\right)^2 + \varepsilon}} \tag{23}$$

The term $0 < \varepsilon \ll 1$ is introduced to prevent the division by zero, whereas α is a regularisation parameter – related to the constraint $\theta_{\max}$ – whose value may be selected empirically[1].

3 NUMERICAL EXPERIMENTS

3.1 Methodology of Experimentation

The synthetic data, used for experimentation, have been generated according to the formula:

$$\tilde{x}_{n,r} = f_k\left(t_n\right) + \Delta\tilde{x}_{n,r} \ \text{ for } n = 1, \ldots, N, \quad r = 1, \ldots, R \text{ and } k = 1, 2 \tag{24}$$

where:

- $f_1(t) \equiv 1 + \frac{2}{3}\left(\exp\left(-\left(\frac{t-3}{3}\right)^6\right)\right)^{12} + \frac{1}{30}t^3$ for $t \in [0, 3]$ is a smooth test function, well suited to be differentiated using Tikhonov regularisation;
- $f_2(t) \equiv \begin{cases} 0.8t & \text{for } t < 1 \\ 0.8 & \text{for } 1 \le t < 2 \\ -0.8(t-3) & \text{for } t \ge 2 \end{cases}$ is a piecewise-linear test function, better suited to be differentiated using TV regularisation;
- $t_n = (n-1)\Delta t$ for $n = 1, \ldots, N = 51$, $\Delta t = 0.06$
- $\Delta\tilde{x}_{n,r}$ are pseudorandom numbers following zero-mean normal distributions whose variances are σ_n^2;
- R is the number of generated sequences of synthetic data, each corresponding to a different set of pseudorandom numbers $\Delta\tilde{x}_{n,r}$ for $n = 1, \ldots, N$ and $r = 1, \ldots, R$.

The functions f_1 and f_2, together with their first derivatives:

$$f_1^{(1)}(t) = -16\left(\exp\left(-\left(\frac{t-3}{3}\right)^6\right)\right)^{12}\left(\frac{t-3}{3}\right)^5 + \frac{1}{10}t^2 \tag{25}$$

$$f_2^{(1)}(t) = \begin{cases} 0.8 & \text{for } t < 1 \\ 0 & \text{for } 1 \le t < 2 \\ -0.8 & \text{for } t \ge 2 \end{cases} \tag{26}$$

are depicted in Figure 2.

[1] The value of the regularisation parameter may significantly influence the quality of the estimates of speed; however, the problem of its selection remains outside the scope of this paper. The interested reader may refer to, *e.g.*, (Hansen, 2010, Chapter 5), (Bauer and Lukas, 2011) and (Reichel and Rodriguez, 2013).

The level of disturbances in the data has been characterised by the signal-to-noise ratio, defined in the following way:

$$SNR_{0,r} \equiv 10\log_{10} \frac{\sum_{n=1}^{N} \left(f\left(t_n\right) \right)^2}{\sum_{n=1}^{N} \left(\tilde{x}_{n,r} - f\left(t_n\right) \right)^2} \quad \text{for } r = 1, \ldots, R \tag{27}$$

The signal-to-noise ratio corresponding to the estimates of the derivative $\hat{x}_{n,r}^{(1)}$ has been determined in the analogous way:

$$SNR_{1,r} \equiv 10\log_{10} \frac{\sum_{n=1}^{N} \left(f^{(1)}\left(t_n\right) \right)^2}{\sum_{n=1}^{N} \left(\hat{x}_{n,r}^{(1)} - f^{(1)}\left(t_n\right) \right)^2} \quad \text{for } r = 1, \ldots, R \tag{28}$$

The performance of the studied methods of numerical differentiation has been compared in terms of the relative signal-to-noise ratio, defined as:

$$RSNR = \frac{1}{R} \sum_{r=1}^{R} \frac{SNR_{1,r}}{SNR_{0,r}} \tag{29}$$

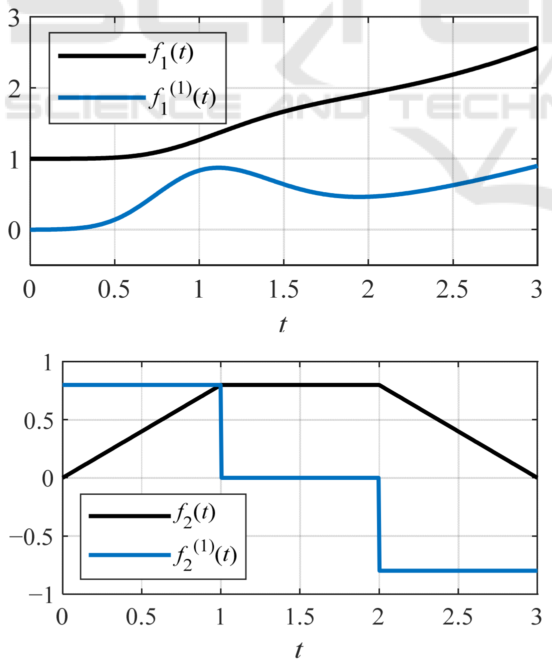

Figure 2: Functions used for the generation of synthetic data and their first derivatives.

The numerical experiments have been designed in such a way as to emulate a monitoring system employing two sensors – called *S1* and *S2* hereinafter – which provide position estimates corrupted with errors whose variances are σ_{S1} and σ_{S2}, respectively, such that:

$$\sigma_{S2} = \psi \sigma_{S1} \quad \text{with} \quad \psi \in [1, 10] \tag{30}$$

Two scenarios have been considered:

- According to the first one – called *scenario #1* hereinafter – S1 and S2 are acquiring data simultaneously; approximately γN data points, uniformly distributed over the time interval under analysis, with $\gamma \in [0.4, 0.8]$, are acquired by means of S2, whereas the remaining data – by S1.
- According to the second one – called *scenario #2* hereinafter – S2 is only acquiring data for $t \in [0.5, \tau]$, with $\tau \in [1.1, 1.7]$, and S1 – only during the remaining fragments of the time interval under analysis. This scenario corresponds to the configuration in which a sensor with low accuracy is used only when the monitored person is outside the field of view of another, more accurate sensor.

Exemplary data, generated according to both above-described scenarios, are shown in Figure 3.

The sequences $\Delta\tilde{x}_{1,r}, \ldots, \Delta\tilde{x}_{N,r}$ have been normalised in order to ensure that $SNR_{0,r}$ remains approximately constant throughout the experimentation, regardless of the ratio σ_{S2}/σ_{S1}:

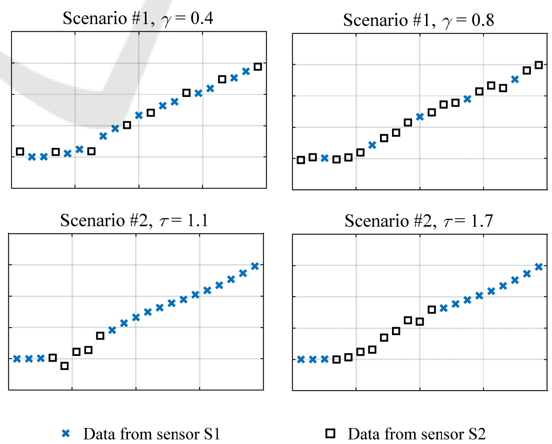

Figure 3: Exemplary data generated according to scenario #1 (first row) and scenario #2 (second row) for different values of γ and τ.

$$\sum_{n=1}^{N}\left(\Delta\tilde{x}_{n,r}\right)^2 \cong N\sigma_{\mathrm{c}}^2 \text{ with } \sigma_{\mathrm{c}} = 0.021 \text{ for } r = 1,\ldots,R \quad (31)$$

The value $\sigma_{\mathrm{c}} = 0.021$ results in $SNR_{0,r} \cong 30$ and is roughly consistent with the authors' previous experiences with impulse-radar sensors and depth sensors (Wagner et al., 2017).

It has been assumed that σ_{S1} is known accurately, *i.e.* that its perfect estimate $\hat{\sigma}_{\mathrm{S1}} = \sigma_{\mathrm{S1}}$ is available; on the other hand, the uncertainty of the estimate $\hat{\sigma}_{\mathrm{S2}}$ of σ_{S2} has been modelled in the following way:

$$\hat{\sigma}_{\mathrm{S2}} = \kappa\sigma_{\mathrm{S2}}, \quad \kappa \in [0.1, 10] \quad (32)$$

For both test functions f_1 and f_2 and for both scenarios, the following experiments have been performed:

- experiments aimed at assessing the influence of the weighting of data on the quality of the speed estimates for different ratios $\sigma_{\mathrm{S1}}/\sigma_{\mathrm{S2}}$, with σ_{S1} and σ_{S2} being known perfectly and the values of all other parameters having been fixed;
- experiments aimed at assessing the influence of the weighting of data on the quality of the speed estimates for different fractions of the data having been acquired by means of sensor S2, with σ_{S1} and σ_{S2} being known perfectly and the values of all other parameters having been fixed;
- experiments aimed at assessing the influence of the ratio $\sigma_{\mathrm{S1}}/\sigma_{\mathrm{S2}}$ on the quality of the speed estimates for different fractions of the data having been acquired by means of sensor S2, with σ_{S1} and σ_{S2} being known perfectly and the values of all other parameters having been fixed;
- experiments aimed at assessing the influence of the error corrupting the estimate $\hat{\sigma}_{\mathrm{S2}}$ of σ_{S2} on the quality of the speed estimates for different ratios $\sigma_{\mathrm{S1}}/\sigma_{\mathrm{S2}}$, with the values of all other parameters having been fixed.

The sequences of data, generated using the test function f_1, have been differentiated using Tikhonov regularisation, whereas those generated using the test function f_2 – using TV regularisation; such a choice is justified by the shapes of those functions. For each sequence of data, the value of the regularisation parameter α has been selected in such a way as to maximise *RSNR*; it is only possible in the synthetic setting of the numerical experiments reported here. This possibility has been exploited in order to study the influence of other parameters on the quality of the speed estimates independently from the influence of the regularisation parameters, although – in practice – the optimisation of regularisation parameters is an important and complex task which, nevertheless, remains outside the scope of this paper.

3.2 Results of Experiments

Figures 4–7 present the results of the numerical experiments described in the previous subsection. In order to facilitate the interpretation of these figures, the symbols of selected parameters, together with their descriptions, are collected in Table 1. The obtained results indicate that:

- The studied method for weighting the data on the basis of the available information about the variances of errors corrupting those data yields an improvement in the quality of the speed estimates when the ratio $\sigma_{\mathrm{S2}}/\sigma_{\mathrm{S1}}$ is sufficiently large, *viz.* larger than *ca.* 2 (*cf.* Figure 4); when that ratio is smaller, the use of $\beta > 0$ does not yield any significant benefit.
- The weighting of data is more advantageous in the case of scenario #2 – *i.e.*, when less accurate data are acquired within a continuous fragment of the time interval under analysis – than in the case of scenario #1 – *i.e.*, when less accurate data are mixed uniformly with more accurate data (*cf.* Figure 4, note the differences in the colour scales).
- In most cases, the values $\beta \in [1,3]$ provide the best results (*cf.* Figure 4).
- In the case of scenario #1, setting β too large yields only modest negative effects (*cf.* Figure 4, left column). On the other hand, in the case of scenario #2, setting β too large may yield results worse than setting $\beta = 0$ – *i.e.*, ignoring the available information about the ratio $\sigma_{\mathrm{S1}}/\sigma_{\mathrm{S2}}$ (*cf.* Figure 4, right column).
- In the case of scenario #2, the dependencies of the quality of the speed estimates on β and on ψ are not significantly affected by the length of the time interval in which the data are acquired by sensor S2 (*cf.* the right columns of Figure 5 and Figure 6).
- In the case of scenario #1 with test function f_2, no systematic dependency of the quality of the speed estimates on the fraction of data acquired

using sensor S2 can be observed in the obtained results (*cf.* the lower-left panels of Figure 5 and Figure 6).

- The quality of the speed estimates is sensitive to the error corrupting the estimate of the variance σ_{S2}^2. In the case of scenario #1 with test function f_1, overestimation of that variance does not increase the errors corrupting the speed estimates as much as its underestimation. On the other hand, in all the other cases, for larger values of that variance the best results are obtained, surprisingly, when it is slightly underestimated (*cf.* Figure 7).

The results presented here are representative examples of the results of a more exhaustive set of experiments, in which other values of the fixed parameters have also been taken into account.

Table 1: Symbols and descriptions of parameters presented in Figures 4–7.

Symbol	Description
β	the amount of weighting of the data according to the estimates of the sensors' accuracy; *cf.* Eq. (14) in Subsection 2.3
γ	in scenario #1, the fraction of the data acquired using sensor S2; *cf.* Subsection 3.1
τ	in scenario #2, the end of the time interval in which data have been acquired using sensor S2; *cf.* Subsection 3.1
ψ	the ratio σ_{S2}/σ_{S1}; *cf.* Subsection 3.1
κ	the relative error corrupting the estimate $\hat{\sigma}_{S2}$ of σ_{S2}; *cf.* Eq. (32) in Subsection 3.1
RSNR	the signal-to-noise ratio in the speed estimates, relative to the signal-to-noise ratio in the measurement data; *cf.* Eq. (29) in Subsection 3.1

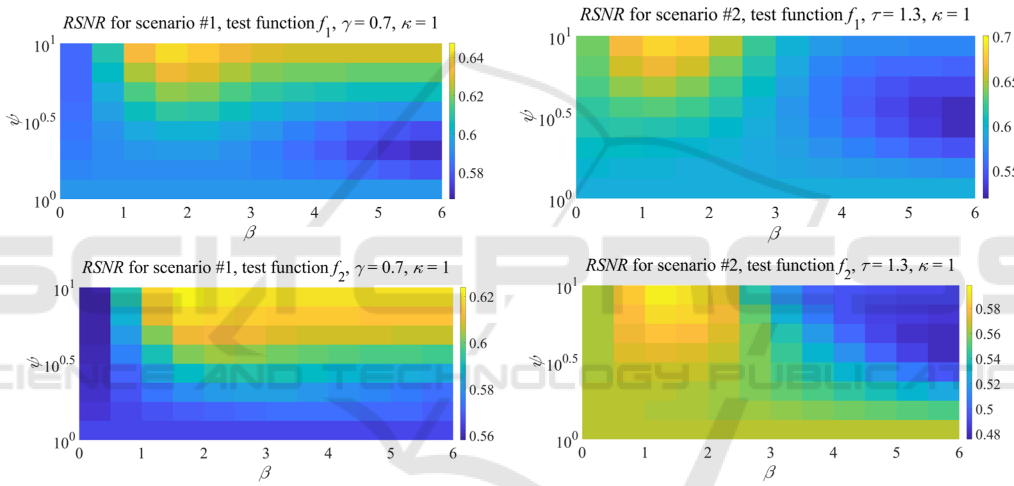

Figure 4: Dependence of *RSNR* on β and ψ for both scenarios, both test functions and fixed values of γ, τ and κ.

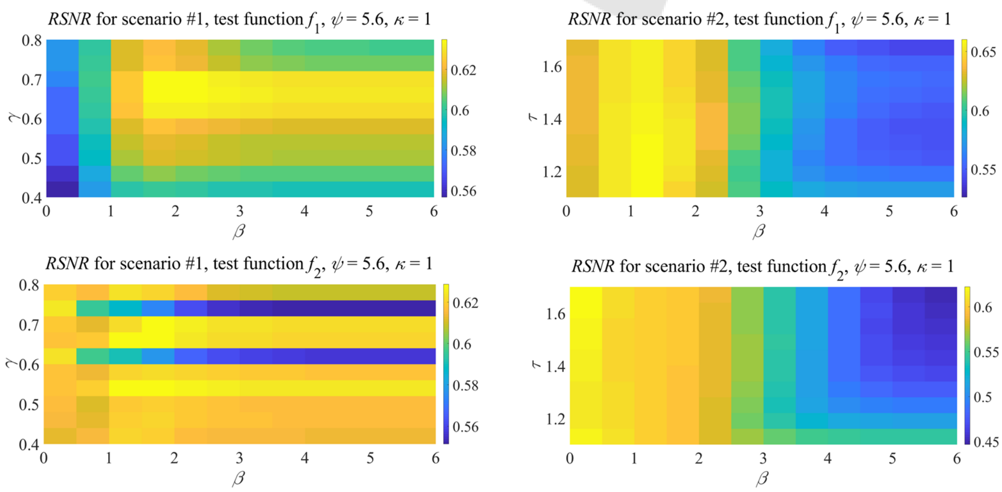

Figure 5: Dependence of *RSNR* on β and γ or τ for both scenarios, both test functions and fixed values of ψ and κ.

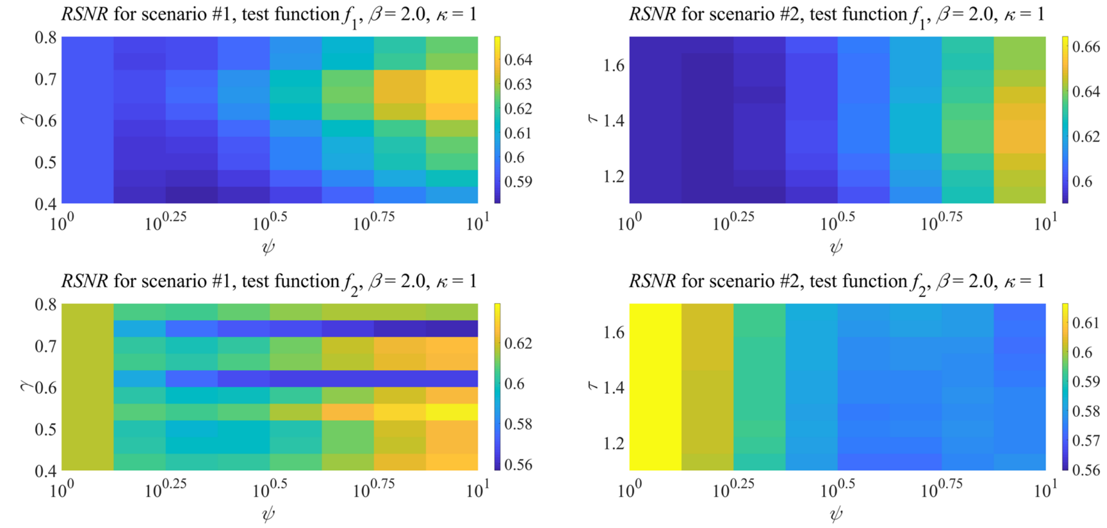

Figure 6: Dependence of *RSNR* on ψ and γ or τ for both scenarios, both test functions and fixed values of β and κ.

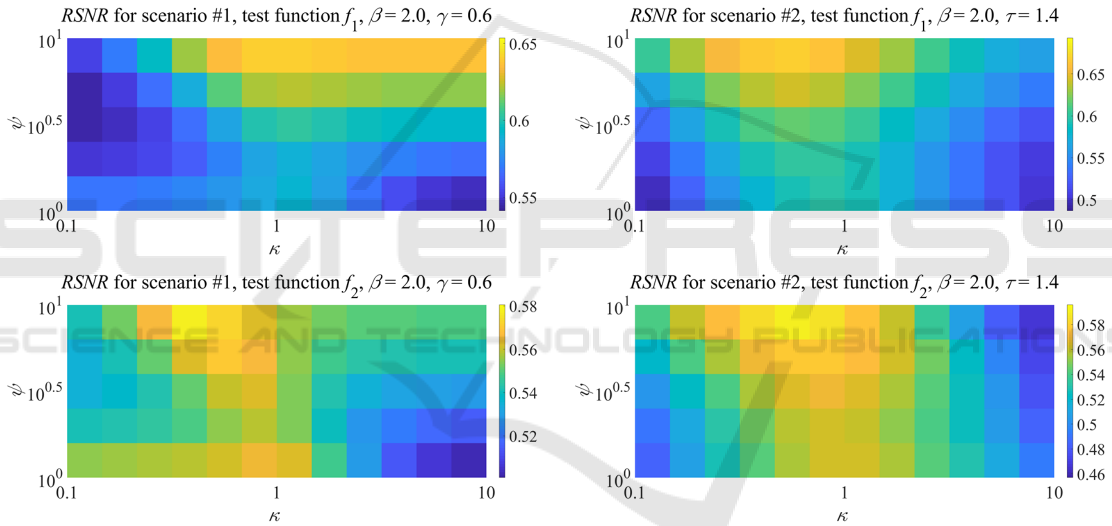

Figure 7: Dependence of *RSNR* on κ and ψ for both scenarios, both test functions and fixed values of β, γ and τ.

4 SUMMARY AND CONCLUSIONS

Healthcare-oriented monitoring systems based on the fusion of data from sensors of various types, which allow for estimating the monitored person's movement speed, may assist healthcare practitioners in their efforts to ensure good quality of life of elderly persons and can contribute to the reduction of the public expenditures related to the healthcare services addressed to those persons.

The technique for fusion of measurement data acquired by means of different sensors, presented in this paper, may be used for improving the accuracy of the estimates of speed obtained using such systems when some *a priori* information about those data is available. Guidelines on the selection of the parameters characterising that technique, based on numerical experimentation, are also provided. These results may turn out to be useful in the development of monitoring systems based on depth sensors and impulse-radar sensors.

The prospects for future studies involve – above all – experiments aimed at testing the described methods on the basis of real-world data.

ACKNOWLEDGEMENT

The work reported in this paper has been accomplished within the project 2017/25/N/ST7/00411 financially supported by the National Science Centre, Poland.

REFERENCES

Al-Shaqi, R., M. Mourshed and Y. Rezgui, 2016. Progress in ambient assisted systems for independent living by the elderly. *SpringerPlus*, vol. 5, no. 1, p. 624.

Baldewijns, G., et al., 2016. Automated in-home gait transfer time analysis using video cameras. *Journal of Ambient Intelligence and Smart Environments*, vol. 8, no. 3, pp. 273–286.

Bauer, F. and M. A. Lukas, 2011. Comparing parameter choice methods for regularization of ill-posed problems. *Mathematics and Computers in Simulation*, vol. 81, no. 9, pp. 1795–1841.

Campos, W., A. Martinez, W. Sanchez, H. Estrada, N. A. Castro-Sánchez and D. Mujica, 2016. A systematic review of proposals for the social integration of elderly people using ambient intelligence and social networking sites. *Cognitive Computation*, vol. 8, no. 3, pp. 529–542.

Chartrand, R., 2011. Numerical differentiation of noisy, nonsmooth data. *ISRN Applied Mathematics*, vol. 2011, pp. 1–11.

Debes, C., A. Merentitis, S. Sukhanov, M. Niessen, N. Frangiadakis and A. Bauer, 2016. Monitoring activities of daily living in smart homes: understanding human behavior. *IEEE Signal Processing Magazine*, vol. 33, no. 2, pp. 81–94.

Fleming, J. and C. Brayne, 2008. Inability to get up after falling, subsequent time on floor, and summoning help: prospective cohort study in people over 90. *BMJ*, vol. 337, p. a2227.

Garcia Marin, J., 2015. *The use of interactive game technology to improve the physical health of the elderly: a serious game approach to reduce the risk of falling in older people*. Ph.D. thesis, Faculty of Engineering and Information Technology, University of Technology, Sydney.

Hagler, S., D. Austin, T. L. Hayes, J. Kaye and M. Pavel, 2010. Unobtrusive and ubiquitous in-home monitoring: a methodology for continuous assessment of gait velocity in elders. *IEEE Transactions on Biomedical Engineering*, vol. 57, no. 4, pp. 813–820.

Hansen, P. C., 2010. *Discrete Inverse Problems: Insight and Algorithms*, Society for Industrial and Applied Mathematics.

Hodgins, D., 2008. The importance of measuring human gait. *Medical Device Technology*, vol. 19, no. 5, pp. 42–47.

Khan, S. S. and J. Hoey, 2017. Review of fall detection techniques: a data availability perspective. *Medical Engineering and Physics*, vol. 39, pp. 12–22.

Kikkert, L. H. J., N. Vuillerme, J. P. van Campen, T. Hortobágyi and C. J. Lamoth, 2016. Walking ability to predict future cognitive decline in old adults: a scoping review. *Ageing Research Reviews*, vol. 27, pp. 1–14.

Lusardi, M., 2012. Is walking speed a vital sign? *Topics in geriatric rehabilitation*, vol. 28, no. 2, pp. 67–76.

Majumder, S., et al., 2017. Smart homes for elderly healthcare—recent advances and research challenges. *Sensors*, vol. 17, no. 11, p. 2496.

United Nations, Department of Economic and Social Affairs, Population Division, 2019. *World population prospects 2019: Highlights. ST/ESA/SER.A/423*. Available: https://population.un.org/wpp/publications (as of October 5, 2020).

Peetoom, K. K. B., M. A. S. Lexis, M. Joore, C. D. Dirksen and L. P. De Witte, 2015. Literature review on monitoring technologies and their outcomes in independently living elderly people. *Disability and Rehabilitation: Assistive Technology*, vol. 10, no. 4, pp. 271–294.

Reichel, L. and G. Rodriguez, 2013. Old and new parameter choice rules for discrete ill-posed problems. *Numerical Algorithms*, vol. 63, no. 1, pp. 65–87.

Rudin, L. I., S. Osher and E. Fatemi, 1992. Nonlinear total variation based noise removal algorithms. *Physica D: Nonlinear Phenomena*, vol. 60, no. 1, pp. 259–268.

Sharkey, A. and N. Sharkey, 2012. Granny and the robots: ethical issues in robot care for the elderly. *Ethics and Information Technology*, vol. 14, no. 1, pp. 27–40.

Shumway-Cook, A., S. Brauer and M. Woollacott, 2000. Predicting the probability for falls in community-dwelling older adults using the Timed Up & Go test. *Physical Therapy*, vol. 80, no. 9, pp. 896–903.

Stickel, J. J., 2010. Data smoothing and numerical differentiation by a regularization method. *Computers & Chemical Engineering*, vol. 34, no. 4, pp. 467–475.

Wada, K., T. Shibata, T. Saito and K. Tanie, 2004. Effects of robot-assisted activity for elderly people and nurses at a day service center. *Proceedings of the IEEE*, vol. 92, no. 11, pp. 1780–1788.

Wagner, J., et al., 2017. Comparison of two techniques for monitoring of human movements. *Measurement*, vol. 111, pp. 420–431.

World Health Organization, 2017. *Integrated care for older people: guidelines on community-level interventions to manage declines in intrinsic capacity*. Available: https://apps.who.int/iris/handle/10665/258981 (as of June 14, 2019).